Microstructure of Poly(1-hexene) Produced by *ansa*-Zirconocenium Catalysis

Gaddam N. Babu and Richard A. Newmark

3M Corporate Research Laboratories, St. Paul, Minnesota 55144

James C. W. Chien*

Department of Polymer Science and Engineering, University of Massachusetts, Amherst, Massachusetts 01003

Received October 15, 1993; Revised Manuscript Received February 28, 1994®

ABSTRACT: Poly(1-hexene) was obtained with *rac*-ethylenebis(1-η^5-indenyl)zirconocenium alkyl catalyst. The ratio of the total proton NMR intensity to the olefinic end group intensity corresponds to the GPC-determined number-average molecular weight. The chemical shift and intensity of the α-CH$_2$ at 34.4 ppm in the ^{13}C NMR spectrum indicate a highly isotactic microstructure for the poly(hexene). The ^{13}C NMR spectra contain minor resonances due to a variety of 1,2-disubstituted and 1,1,2-trisubstituted vinylene and vinylidene end groups.

I. Introduction

1-Hexene is an α-olefin extensively used as a comonomer in linear low-density poly(ethylene) (LLDP). A large body of data on the copolymerization of ethylene with hexene and on the properties of the LLDP formed probably exists in industrial research laboratories. The advent of metallocene catalysts had the most immediate impact on the manufacture of LLDP, because they produced materials of greatly improved toughness, i.e., dart puncture strength, relative to copolymers made with the heterogeneous TiCl$_3$ catalyst. It is important to understand the causes of this difference and whether it is due to the physical states of the catalysts or the number of catalytic sites.

One poorly understood copolymerization phenomenon is the "comonomer effect", where an α-olefin comonomer greatly accelerates the rate of copolymerization with ethylene. We have compared the ethylene-hexene copolymerization by heterogeneous and homogeneous Ziegler-Natta catalysts to aid in the understanding of the comonomer effect.[1] It was found that this effect was pronounced for low-activity TiCl$_3$ catalyst but was absent in copolymerizations by zirconocene catalysts. The comonomer effect could contribute toward more homogeneous comonomer distributions in the copolymers obtained with the zirconocene catalysts. The products of reactivity ratios in ethylene-α-olefin copolymerization differ significantly between these catalysts:[2] the values are less than unity for the new homogeneous metallocene catalysts but are greater than unity for the heterogeneous TiCl$_3$ catalyst and the zirconocene catalyst.[3] The systems were found to be comparable in their optimum catalytic productivities. The polymer produced by the former is much higher in molecular weight (MW) than the latter.

The purpose of this study is to determine the microstructures of the poly(1-hexene) obtained with the homogeneous catalyst and to understand the different types of termination reactions.

II. Experimental Section

rac-Ethylenebis(1-η^5-indenyl)dichlorozirconium (1)[4] and triphenylcarbenium tetrakis(pentafluorophenyl)borate (2)[5] were synthesized by published procedures. Polymerization of 1-hexene was carried out at temperatures (T_p) of -30, 0, and 25 °C; the products are designated as PH(-30), PH(0), and PH(25), respectively.

Zirconocenium ion (1$^+$) was generated *in situ* by the reaction of 1 (12 μM) with triethylaluminum (TEA, Aldrich, 1 mM) and 2 (12 μM) in the presence of 1 M 1-hexene (4 g in 47 mL of toluene) up to 6.7 M. The excess of TEA is required to scavenge impurities in the polymerization reactor. The products were worked up with acidic methanol, washed with methanol, and evacuated to remove residual toluene and methanol.

NMR spectra were obtained in CDCl$_3$ solution at +22 °C. The spectrum of PH(25) was also run in 1,2,4-trichlorobenzene at 110 °C but was found to exhibit lower resolution than at ambient temperature in CDCl$_3$. Additional high-temperature spectra were not acquired. Proton spectra were obtained on a UNITY 500 NMR spectrometer operating at 500.0 MHz with 15° (2.4 μs) pulses, 3.0-s acquisition time, and 8-kHz sweep width. The ^{13}C NMR spectra were obtained on the UNITY 500 at 125.7 MHz with full nuclear Overhauser enhancement, 75° (7.8 μs) pulses, 0.8-s acquisition time, and 26.4-kHz sweep width. Approximately 40 000 transients were obtained for each sample in 8 h. Relaxation times were measured using the usual 180°-τ-90° pulse sequence. Spectra were acquired for seven values of τ ranging from 0.2 to 2 s. Relaxation times were <0.15 s for the backbone and α carbons and were 0.33, 0.7, and 1.4 s for the β, γ, and δ positions from the backbone for the butyl side chain. Quantitative ^{13}C spectra must be obtained with suppression of the nuclear Overhauser effect and relaxation delays of 5T_1. However, these conditions would require over a week of spectrometer time for each spectrum. It is only possible to obtain qualitative spectra with continuous decoupling and no relaxation delay in a reasonable time frame (8 h for each spectrum in Figures 2-4). If we assume relaxation times in the end groups are similar to those observed in the side chains, then the observed relaxation times of the butyl side chains indicate that the overnight ^{13}C spectra, run with 0.8-s acquisition times and 75° pulses, should show almost full intensities for the backbone carbons and for carbons at least two carbons in from the end groups.

Molecular Weight Determination. Gel permeation chromatographic analyses of polymers were performed at a flow rate of 1.0 mL/min in tetrahydrofuran at 30 °C using a Waters HPLC component system (RI detector) equipped with six ultra-μ-Styragel columns (two 500, two 10^3, 10^4, and 10^5 Å) after calibration with standard polystyrene samples from Polymer Laboratories. Molecular weight determinations were done on a Hewlett-Packard computer with software supplied by the Nelson Analytical Co.

III. Results

The full proton spectrum of PH(25) is shown in Figure 1. The high-gain insets in the figure correspond to the resonances from the end groups for PH(-30), PH(0), and PH(25). The geminal protons in the RR′C=CH$_2$ end group are inequivalent because one is cis to a butyl group

---

® Abstract published in *Advance ACS Abstracts*, May 1, 1994.

0024-9297/94/2227-3383$04.50/0

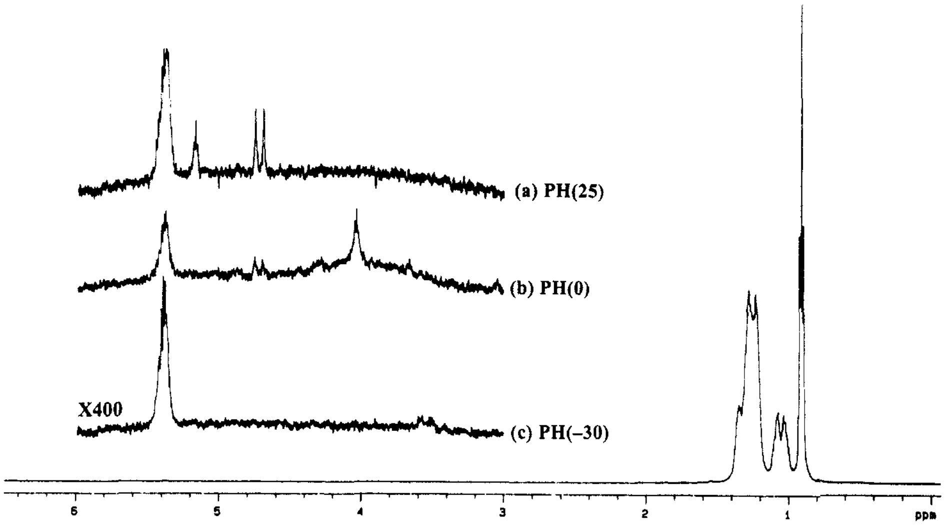

Figure 1. ^{1}H NMR spectrum of PH(25). Insets are high-gain (×400) spectra between 6 and 3 ppm of PH(25), PH(0), and PH(−30).

Table 1. Proton NMR Mole Ratios of the End Groups and $\bar{M}_n$

	proton NMR mole ratios						
sample	$RR'C{=}CH_2$ (δ 4.6, 4.7)	$RCH{=}CHR'$ (δ 5.3)	$RCH{=}CR'R''$ (δ 5.1)	R_2CHOH/RCH_2OH (δ 3.5–4.0)	$\bar{M}_n$(NMR)	$\overline{DP}_n$	$\bar{M}_n$(GPC)
PH(−30)	0	92	0	8	23 300	300	26 800
PH(0)	8	40	7	46	18 400	410	25 900
PH(25)	12	66	22	0	15 200	180	

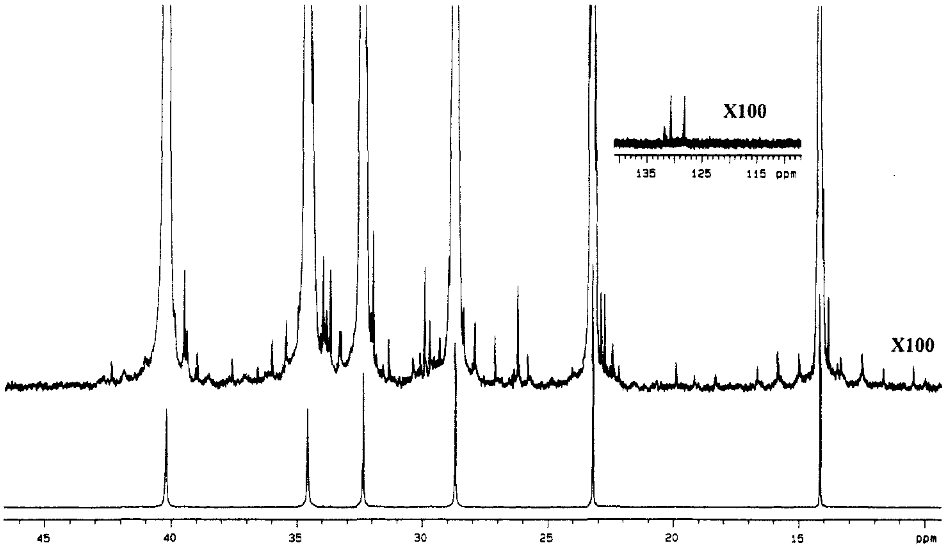

Figure 2. ^{13}C NMR spectrum of PH(−30) obtained in 8 h with a 0.8-s acquisition time, 7.8-μs (75°) pulse width, no relaxation delay, and proton Waltz decoupling.

and the other is cis to the polymer chain. These two protons have chemical shift values of 4.62 and 4.69 ppm. The internal olefinic protons resonate at 5.1 and 5.3 ppm for $RR'C{=}CHR''$ and $RCH{=}CHR'$, respectively.[6b] Weak absorptions were also present at 3.4 and 3.9 ppm in the PH(−30) and PH(0) samples but were virtually absent in the PH(25) material. They may be attributed to methyleneoxy (RCH_2OH) and/or methylidyneoxy protons. These protons are assumed to be the end groups which result from the exposure of oxygen to the carbon–Al bonds during workup. The proton NMR shows no absorption in the region near 5.8 ppm for the olefinic CH in a $-CH_2-CH{=}CH_2$ end group. Therefore, there are few if any vinyl end groups.

Normalized mole ratios of the olefinic and methyleneoxy end groups of the polymers were determined from the analysis of the end group proton NMR intensities. The results are listed in Table 1. Number-average molecular weights ($\bar{M}_n$) are calculated from the integration of the major polyhexene absorption (12H) in the proton NMR relative to the sum of the end group absorptions (1 and 2H depending on the end group). The $\bar{M}_n$ values are in reasonable agreement with $\bar{M}_n$ values obtained by GPC considering the poor signal/noise in the proton spectra.

The ^{13}C NMR spectra of the poly(1-hexenes) are shown in Figures 2–4. Failure to observe the oxy carbons in the ^{13}C NMR between 60 and 70 ppm must be due to peak broadening from a number of similar, but not identical, oxy carbon end groups. The chemical shift intensity of the α-CH_2 at 34.4 ppm indicates the polymers are highly isotactic; the α-CH_2 in atactic and syndiotactic triads occurs between 0.4 and 1.0 ppm upfield from 34.4 ppm.[7]

Chemical shifts of the six major resonances have been estimated using two different methods.[9,10] Calculated values using the CSPEC program by Cheng[9] are based on the Grant and Paul[10] additivity rules for hydrocarbon

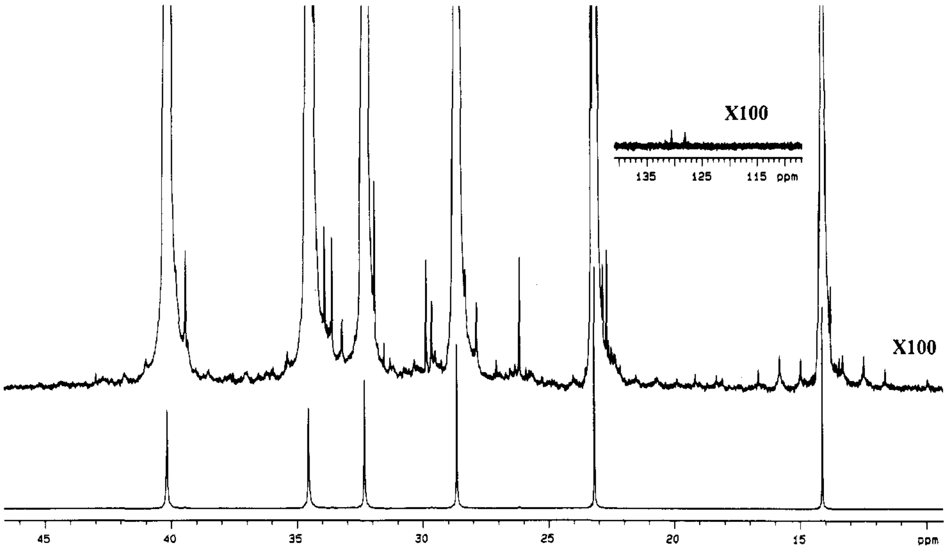

Figure 3. ^{13}C NMR spectrum of PH(0), run under the same conditions as Figure 2.

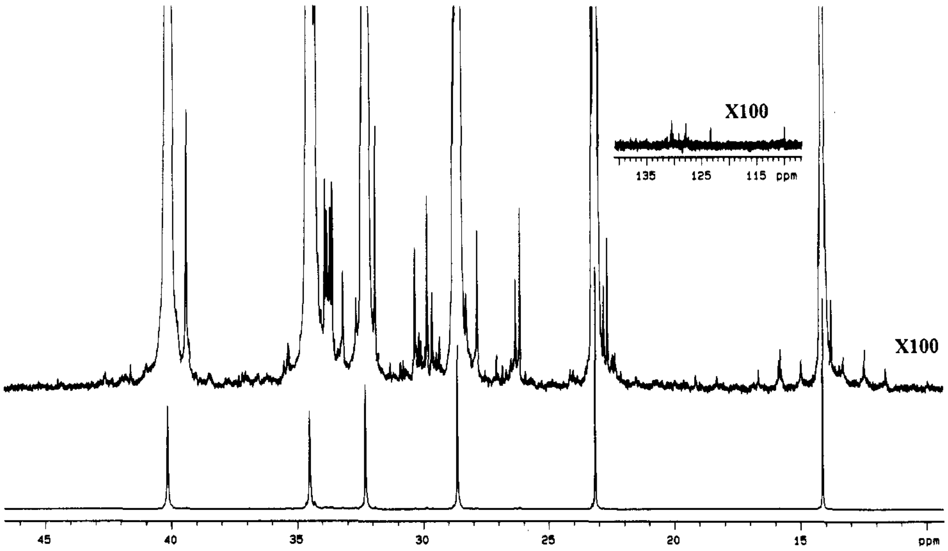

Figure 4. ^{13}C NMR spectrum of PH(25), run under the same conditions as Figure 2.

substituents. The second set of calculated shifts is from the spectral estimation feature of the SPECINFO database.[11] This program calculates chemical shifts based on a comparison of the given structure to carbons in the database which have the most similar substituents α, β, γ, and δ carbons from the carbon of interest.

$$\{CH_2{-}CH{-}(CH_2{-}CH_2{-}CH_2{-}CH_3)\}_n$$

CSPEC calc[9]	40.3	31.1	35.3	30.3	23.4	14.0
SPECINFO calc[11]	43.4	33.8	33.9	29.2	23.0	14.1
obsd	40.2	32.4	34.4	28.7	23.2	14.2

(1)

Comparison of the calculated and observed values shows the empirical values from the SPECINFO database are better for some carbons, while the calculated values based on additivity effects fare better for others. The estimated errors for the SPECINFO calculation are mostly under 1 ppm, except for the CH_2 α to the backbone, for which the error is 4 ppm. The failure of SPECINFO to give good values indicates the absence of carbons with almost identical substituents in the database.

Numerous minor absorptions are observed in the carbon spectra. All the minor absorptions in the carbon-13 spectrum are under 2% of the intensity of the major peaks, and most are only 1%. Several of the stronger minor absorptions are identical in the three samples, but many of the minor resonances show considerable variations in intensity. The chemical shifts and relative intensities of the strongest of the minor peaks are given in Table 2. A DEPT spectrum[8] (Figure 5) was obtained on the PH(−30) sample. It showed that the very minor absorptions between 5 and 22 ppm were methyl groups whereas all the remaining peaks were methylene except the backbone CH at 32.3 ppm and the minor resonances at 35.43 and 35.99 ppm. The minor olefinic absorptions must be attributed to various types of terminal unsaturation. The latter suggests different end groups were formed depending on the T_p. This is consistent with the proton spectra, which also show different end groups. The several terminal unsaturation signals between 132 and 110 ppm indicate different sequence arrangements of nearest-neighbor units. The concentration of the different types of unsaturated end groups is dependent on T_p. Lowering T_p increased the concentration of 1,2-disubstituted unsaturation relative to other types of end groups (Table 1).

Very weak absorptions near 20 ppm are probably due to the presence of methyl end groups, but these are insignificant compared to the olefinic end groups and the minor absorptions in the carbon spectrum. The origin of

Table 2. Intensities of Minor Peaks in the ^{13}C NMR of Poly(1-hexenes)

chem shift (ppm)	multiplicity	% of total intensity[a] PH(25)	PH(0)	PH(−30)
131.72	CH	0.06	0.02	0.06
131.40	CH	0.03	0.02	0.03
130.77	CH	0.04		
130.58	CH	0.11	0.06	0.20
130.29	CH	0.03		
129.33	CH	0.06		
128.24	CH	0.04	0.03	0.08
128.11	CH	0.04	0.04	0.14
123.47	CH	0.03		
110.14	CH_2	0.05		
39.48	CH_2	1.75	0.38	0.98
39.37	CH_2		0.03	0.47
38.98	CH_2			0.22
35.99	CH			0.14
35.43	CH			0.25
33.96	CH_2	0.56	0.31	0.29
33.90	CH_2	0.83	0.03	0.05
33.83	CH_2	0.56		0.10
33.76	CH_2	0.56		0.05
33.67	CH_2		0.44	0.37
33.31	CH_2			0.14
33.25	CH_2	0.42	0.14	0.17
31.34	CH_2			0.22
30.34	CH_2	0.56		0.17
30.09	CH_2			0.10
29.91	CH_2	0.78	0.28	0.42
29.69	CH_2	0.22	0.28	0.20
29.30	CH_2			0.10
27.91	CH_2	0.78	0.36	0.34
27.12	CH_2			0.14
26.38	CH_2	0.72		0.14
26.19	CH_2	0.67	0.33	0.42
25.81	CH_2			0.12

[a] The accuracy is about 20% due to overlap of the minor peaks with the tails of the major absorptions. Intensities are from spectra obtained with 75° pulses and 0.8-s acquisition times. No corrections have been made for differences in relaxation times or nuclear Overhauser effects.

methyl end groups may be from the initial step or may arise from σ-bond metathesis according to the reaction mechanism proposed below.

Absorption in the region 25.4–26.4 ppm, present in all spectra in <1% concentration, is attributed to methylene carbon chemical shifts as indicated in Schemes 1, 2, and 4.

IV. Discussion of Results

The microstructure of a macromolecule is a record of the chemical events which took place during its formation. The end groups reflect the chain initiation and termination processes. The zirconocenium species was produced by the following reactions:[4]

$$\mathrm{Et(Ind)_2ZrCl_2 + 2AlEt_3 \rightarrow Et(Ind)_2ZrEt_2 + 2AlEt_2Cl} \quad (2)$$

$$\mathrm{Et(Ind)_2ZrEt_2 + (C_6H_5)_3C^+B^-(C_6F_5)_4 \rightarrow \underset{3}{Et(Ind)_2Zr^+Et} + B^-(C_6F_5)_4 + (C_6H_5)_3CEt} \quad (3)$$

Therefore, some of the chains may contain an Et end group.

$$\mathrm{Et(Ind)_2Zr^+Et + \mathit{n}CH_2{=}CHR \rightarrow Et(Ind)_2Zr^+{-}CH_2{-}CHR{-}Et} \quad (4)$$

However, the number of such Et end groups would be quite small. In a typical hexene polymerization, 6.25 × 10^{-7} mol of 1^+ produced about 2 g of PH with an $\bar{M}_n$ of about 2 × 10^4 or about 10^{-4} mol of PH molecules. This corresponds to 160 chains produced by each 1^+. Most of the chains were in fact initiated by $Et(Ind)_2Zr^+H$ (4)[6],

$$\mathrm{\underset{4}{Et(Ind)_2Zr^+H} + \mathit{n}CH_2{=}CHR \rightarrow Et(Ind)_2Zr^+{-}(CH_2{-}CHR)_{\mathit{n}}{-}H} \quad (5)$$

Species 4 is formed by the βH elimination

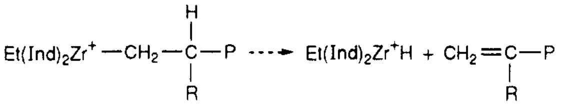

$$\mathrm{Et(Ind)_2Zr^+{-}CH_2{-}\overset{H}{\underset{R}{C}}{-}P} \dashrightarrow \mathrm{Et(Ind)_2Zr^+H + CH_2{=}\underset{R}{C}{-}P} \quad (6)$$

This well-known chain transfer process, eq 6 followed by eq 5, is facilitated by the electrophilic zirconium center and the electron-donating effect of the β-butyl group. The importance of the latter contribution can be seen in ethylene polymerization. In this case the βH elimination is sufficiently slow to enable the competing σ-bond metathesis manifest[6]

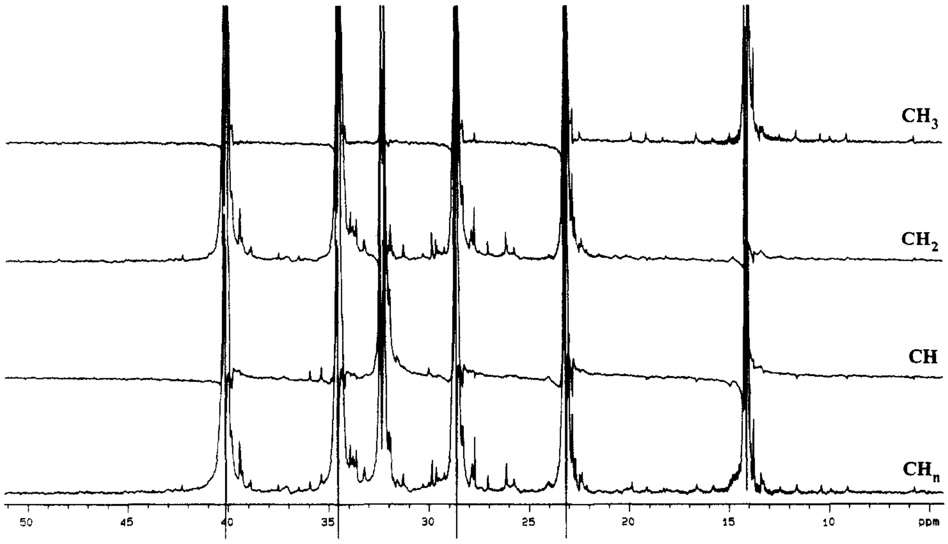

Figure 5. Edited DEPT spectra of PH(−30) plotted at high gain to show multiplicities of the end groups. Each DEPT spectrum was obtained in 3.5 h with a 0.4-s acquisition time, 1.0-s delay, and Waltz decoupling during the acquisition.

$$\mathrm{Et(Ind)_2Zr^+{-}CH_2CH_2{-}P + CH_2CH_2 \rightarrow Et(Ind)_2Zr^+{-}CH{=}CH_2 + PCH_2CH_3} \quad (7)$$

There is no significant absorption near 11 ppm in the ^{13}C NMR spectra where methyls of a $CHBuCH_2CH_3$ end group should be observed. This is consistent with the dominance of βH elimination (eq 6) over σ-bond metathesis (eq 7) in 1-hexene polymerization.

If all the monomers are inserted via the primary mode, i.e., 1,2-addition, and the chains are terminated by βH elimination, then vinylidene would be the prevailing olefinic group. In fact, the most abundant group is the 1,2-trisubstituted olefins (Table 1).

The complexity of the ^{13}C NMR spectra indicates that there are several types of vinylene groups. This can be attributed to the migration of the Zr moiety along the carbon backbone.[12] Scheme 1, with R = ethyl and P = polymer chain, shows the process along the main chain to form the various isomeric zirconocenium (**a**) and subsequently the 1,1,2-trisubstituted vinylenes (**b2, b3, b4**) via βH eliminations. We have estimated the chemical shifts for the olefinic and α and β aliphatic carbons using the CSPEC calculation for **b1**–**b4**. The results are given on the structures in Scheme 1. Chemical shifts were also estimated using the SPECINFO calculation, but the program-estimated errors were between 3 and 5 ppm for many of the carbons. These large values indicate that the database does not have suitable references for this calculation (vide supra). Since the CSPEC calculation is strictly empirical based on substituents, its errors should be similar to those observed for polyhexene, except for the backbone methylene carbons for which the error is larger because the steric contribution to the chemical shift in the backbone methine is not calculated accurately (this is reflected in the calculation not including any effects due to tacticity).

Analogous processes involving the pendant group are depicted in Scheme 2 in which the zirconium cation undergoes isomerization first from **1a** to **2a** (Scheme 1) followed by its migration along the chain to the least hindered site, i.e., the terminal carbon, C5, as shown in Scheme 2. This leads to 1,2-disubstituted vinylenes **d2** and **d3** as well as the trisubstituted olefin **d1**. The vinylene groups are represented by **d1** and **d4**. The above migrations have to compete against the normal propagation. The formation of trisubstituted olefins (**f1**) may also originate from the addition of 1-hexene in the 2,1 mode (misinsertion) to the propagating chain as shown in Scheme 3. Isomerization of **e3** to other isomers (Scheme 4) occurs by analogy to Schemes 1 and 2, yielding structures **f1**–**f7**. This process does not involve the formation of zirconium on a tertiary carbon. The important chemical shifts due to unsaturated carbons and other carbons around the unsaturation are also given in Schemes 2 and 4 using the CSPEC calculation.

Scheme 1

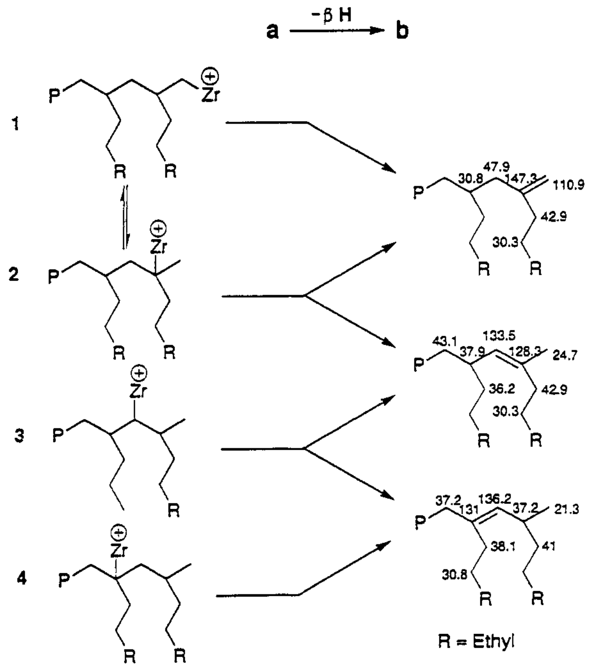

Scheme 2

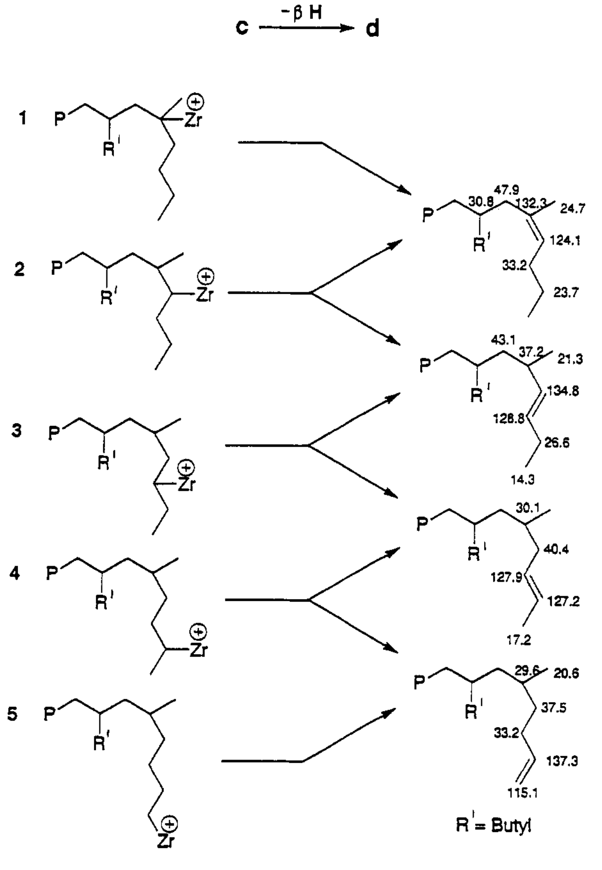

In the case of propylene polymerization catalyzed by (ethylene)bis(4,5,6,7-tetrahydro-1-η^5-indenyl)dichlorozirconium/methylaluminoxane,[13] there is 1 secondary monomer insertion for every 200 primary monomer insertions. Molecular mechanics calculations[14] showed that following a secondary insertion, the subsequent monomer insertion via any mode becomes prohibitively slow because of a several kcal/mol increase in steric energy. In other words, chain growth is effectively stalled. For instance, βH elimination and reinsertion can form a tetramethylene sequence[4b,15] in propylene polymerization. In the present case, a misinsertion-stalled polymerization would allow the zirconocenium moiety migration to occur as in Schemes 1, 2, and 4 to produce additional varieties of unsaturations observed for the poly(1-hexenes).

The presence of hydroxy groups is not unexpected. They may be produced by reactions such as

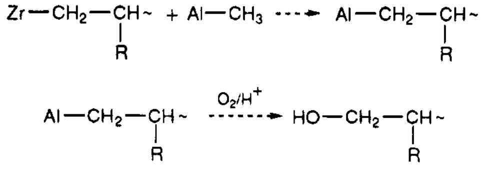

$$\mathrm{Zr{-}CH_2{-}\underset{R}{CH}\sim + Al{-}CH_3 \dashrightarrow Al{-}CH_2{-}\underset{R}{CH}\sim}$$

$$\mathrm{Al{-}CH_2{-}\underset{R}{CH}\sim \xrightarrow{O_2/H^+} HO{-}CH_2{-}\underset{R}{CH}\sim} \quad (8)$$

The ^{13}C NMR spectra of PH(0) and PH(25) showed

Scheme 3

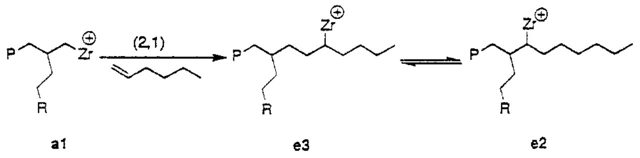

Scheme 4

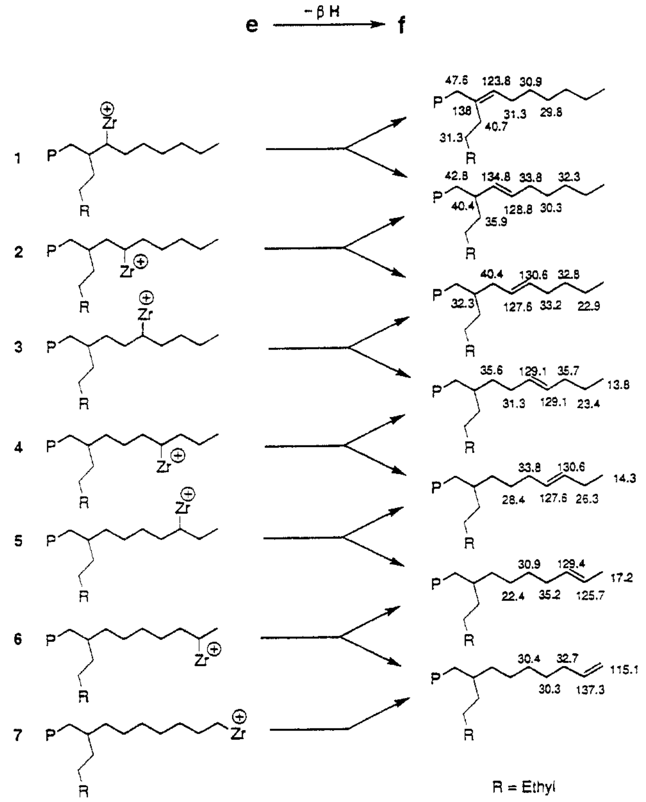

absorptions at 124, 128, 131, and 134 ppm, due to trisubstituted olefins. The formation of such structures has been shown in Schemes 1–4. According to Scheme 1, the migration may be occurring along the backbone to account for the trisubstituted olefinic carbons. We believe that this is not a dominant process since the migration of the zirconium cation has to occur from a secondary carbon to a tertiary carbon, which is unlikely on energy considerations. End group **b1** is most readily observed in the proton NMR (Table 1),[6a] and the ^{13}C CH_2 absorption at 110.1 ppm is clearly assigned to this structure. The quaternary carbon should be near 147.3 ppm, but it is too weak to observe. Vinyl end groups, as in **d4** or **f7**, are not observed in the proton NMR and must be negligible. The calculated chemical shifts for the olefinic and aliphatic carbons in **f1–f6** and **d1–d3** are consistent with the observed chemical shifts reported in Table 2. However, the limited accuracy of the calculated shifts and the plethora of end group resonances preclude making unambiguous assignments at this time.

Acknowledgment. This work was supported in part by the Materials Research Laboratories of the National Science Foundation at the University of Massachusetts, Amherst, MA.

References and Notes

(1) Chien, J. C. W.; Nozaki, T. *J. Polym. Sci., Part A* **1993**, *31*, 227.
(2) Chien, J. C. W., unpublished data.
(3) Chien, J. C. W.; Gong, B. M. *J. Polym. Sci., Part A* **1993**, *31*, 1747.
(4) (a) Wild, F. R. W. P.; Zsolorai, L.; Huffner, G.; Brintzinger, H. H. *J. Organomet. Chem.* **1982**, *232*, 233. (b) Rieger, B.; Mu, X.; Mallin, D. T.; Rausch, M. D.; Chien, J. C. W. *Macromolecules* **1990**, *23*, 3559.
(5) (a) Chien, J. C. W.; Tsai, W. M.; Rausch, M. D. *J. Am. Chem. Soc.* **1991**, *113*, 8570. (b) Tsai, W. M.; Rausch, M. D.; Chien, J. C. W. *Appl. Organomet. Chem.* **1993**, *7*, 71. (c) Chien, J. C. W.; Tsai, W. M. *Makromol. Chem., Macromol. Symp.* **1993**, *66*, 141.
(6) (a) Siedle, A. R.; Lamanna, W. M.; Olofson, J. M.; Nerad, B. A.; Newmark, R. A. ACS Symposium Series 159; American Chemical Society: Washington, DC, 1993; Chapter 11, p 156. (b) Lamanna, W. M., private communication.
(7) Asakura, T.; Demura, M.; Nishiyama, Y. *Macromolecules* **1991**, *24*, 2334.
(8) Pegg, D. T.; Doddrell, D. M.; Brooks, W. M.; Bendall, M. R. *J. Magn. Reson.* **1981**, *44*, 32.
(9) Cheng, H. N.; Bennett, M. A. *Anal. Chim. Acta* **1991**, *242*, 43.
(10) Paul, E. G.; Grant, D. M. *J. Am. Chem. Soc.* **1964**, *86*, 2984.
(11) SPECINFO database in STN, available from Chemical Abstracts Service, Columbus, OH.
(12) Schwartz, J.; Labinger, J. A. *Angew. Chem.* **1976**, *15*, 333.
(13) Tsutsni, T.; Mizuno, A.; Kashiwa, N. *Makromol. Chem.* **1989**, *190*, 1177.
(14) Yu, Z. T.; Chien, J. C. W. *J. Am. Chem. Soc.*, submitted.
(15) Following a 2,1-insertion of propylene, the elimination of a hydrogen from the β-methyl group followed by reinsertion introduces a tetramethylene sequence observed by ^{13}C NMR.

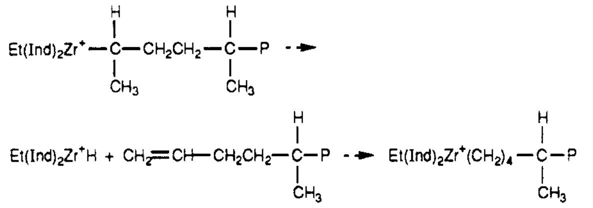

$$Et(Ind)_2Zr^+\text{—}\underset{CH_3}{\overset{H}{C}}\text{—}CH_2CH_2\text{—}\underset{CH_3}{\overset{H}{C}}\text{—}P \rightarrow$$

$$Et(Ind)_2Zr^+H + CH_2\text{=}CH\text{—}CH_2CH_2\text{—}\underset{CH_3}{\overset{H}{C}}\text{—}P \rightarrow Et(Ind)_2Zr^+(CH_2)_4\text{—}\underset{CH_3}{\overset{H}{C}}\text{—}P$$